Radar-rainfall estimation algorithms of Hydro-NEXRAD

Bong-Chul Seo, Witold F. Krajewski, Anton Kruger, Piotr Domaszczynski,
James A. Smith and Matthias Steiner

ABSTRACT

Hydro-NEXRAD is a prototype software system that provides hydrology and water resource communities with ready access to the vast data archives of the U.S. weather radar network known as NEXRAD (Next Generation Weather Radar). This paper describes radar-rainfall estimation algorithms and their modular components used in the Hydro-NEXRAD system to generate rainfall products to be delivered to users. A variety of customized modules implemented in Hydro-NEXRAD perform radar-reflectivity data processing, produce radar-rainfall maps with user-requested space and time resolution, and combine multiple radar data for basins covered by multiple radars. System users can select rainfall estimation algorithms that range from simple ('Quick Look') to complex and computing-intensive ('Hi-Fi'). The 'Pseudo NWS PPS' option allows close comparison with the algorithm used operationally by the US National Weather Service. The 'Custom' algorithm enables expert users to specify values for many of the parameters in the algorithm modules according to their experience and expectations. The Hydro-NEXRAD system, with its rainfall-estimation algorithms, can be used by both novice and expert users who need rainfall estimates as references or as input to their hydrologic modelling and forecasting applications.

Key words | Hydro-NEXRAD, precipitation, radar-rainfall

Bong-Chul Seo
Witold F. Krajewski (corresponding author)
Anton Kruger
Piotr Domaszczynski
IIHR-Hydroscience and Engineering,
The University of Iowa,
Iowa City, IA 52242,
USA
E-mail: *witold-krajewski@uiowa.edu*

James A. Smith
Department of Civil and
  Environmental Engineering,
Princeton University,
Princeton, NJ 08544,
USA

Matthias Steiner
National Center for Atmospheric Research,
Boulder, CO 80301,
USA

INTRODUCTION

This paper focuses on radar-rainfall estimation algorithms and their modular components used in the Hydro-NEXRAD software system (Krajewski *et al.* 2011; Kruger *et al.* 2011). In this context, a 'module' is defined as an individual executable component for processing data and an 'algorithm' denotes an appropriate combination of modules used to produce radar-rainfall estimates, that is, the main products of the system. The creation of the system was motivated by the need to increase the use of NEXRAD data in hydrologic research. Accessing and processing the basic data, known as Level II data, is cumbersome and requires substantial experience and expertise so many researchers limit themselves to the readily available hourly rainfall accumulation maps, with approximately 4×4 km^2 spatial resolution, provided by the National Weather Service (NWS). However, use of Level II data allows for the creation of products with higher spatial and

temporal resolution, thus expanding the range of applications. Hydro-NEXRAD provides hydrologic users who lack weather radar experience with data access to create such customized products quickly and conveniently.

The creation of Hydro-NEXRAD required the development of a number of data-processing modules and implementation of the algorithms documented in the literature. In the paper we categorize them as follows: (1) processing radar reflectivity data; (2) converting reflectivity to rainfall; and (3) merging data from multiple radars. All of these categories have received considerable attention in the literature (e.g. Battan 1973; Zawadzki 1982; Austin 1987; Rosenfeld *et al.* 1994; Smith *et al.* 1996; Zhang *et al.* 2005). Our objective is not to propose a new set of radar-rainfall estimation algorithms. Rather, it is to document how we define different Hydro-NEXRAD system modules, discuss how they are organized

together in the system, and document their advantages and shortcomings. Some of these modules include our modifications and improvements, but our focus here is on describing radar-rainfall estimation algorithms that produce rainfall maps delivered to users and completing the description of the Hydro-NEXRAD system given in Krajewski *et al.* (2011) and Kruger *et al.* (2011). A future study will comprehensively detail the Hydro-NEXRAD algorithms' performance.

Processing reflectivity data

Radar collects three-dimensional (3D) reflectivity data in a polar coordinate system which is referred to as a full volume scan (e.g. Battan 1973; Doviak & Zrnic 1993). Radar reflectivity data are contaminated by numerous error sources (e.g. Zawadzki 1982; Austin 1987; Smith *et al.* 1996) and require careful processing prior to their use in quantitative precipitation estimation (QPE). As radar echo may originate from both atmospheric and ground-based targets, reflectivity data requires classification. While ground clutter due to side lobes' interactions with the terrain near the radar site is rather straightforward, the detection and elimination of echoes that arise due to anomalous propagation (AP) conditions in the atmosphere (e.g. Battan 1973) are more difficult to automate. Numerous approaches addressing this problem have been proposed in the literature (e.g. Moszkowicz *et al.* 1994; Grecu & Krajewski 2000; Kessinger *et al.* 2003; Ellis *et al.* 2003; Berenguer *et al.* 2006; Cho *et al.* 2006; Lakshmanan *et al.* 2007). In Hydro-NEXRAD, we adapt Steiner & Smith's (2002) approach, which works by analyzing the vertical and horizontal echo structure in a 3D vicinity of a given pixel.

Reflectivity data collected from regions far from the radar site represent a biased view of the near-ground precipitation. The systematic aspect of this misrepresentation can be corrected to some extent. Such range effect correction can be applied to the reflectivity data classified as meteorological echoes. The correction procedures account for the bright band, that is, enhanced reflectivity value associated with the melting snow (Austin & Bemis 1950; Kitchen *et al.* 1994; Fabry & Zawadzki 1995; Gourley & Calvert 2003; Zhang *et al.* 2008) and/or the systematic weakening of the radar echo with height (e.g. Kitchen *et al.* 1994; Andrieu & Creutin 1995; Joss & Lee 1995; Vignal *et al.* 1999; Seo *et al.* 2000; Vignal & Krajewski 2001; Chumchean *et al.* 2004). In Hydro-

NEXRAD, we implemented a range-correction module originally proposed by Vignal *et al.* (1999) and adapted to WSR-88D (radars used in the NEXRAD system) data by Vignal & Krajewski (2001).

As volume scan data are inconvenient to analyze and convert into rainfall products, one can construct two-dimensional (2D) reflectivity maps (e.g. Battan 1973; Fulton *et al.* 1998) as simple single scans for a given radar antenna elevation angle (known as a plan position indicator (PPI)) or a combination of data from different antenna elevation angle scans (known as a hybrid scan). Both options are available in Hydro-NEXRAD.

Converting reflectivity to rainfall

A Z–R (power–law relationship) relationship must be applied to convert radar reflectivity data to rainfall rate. This relationship can be derived from the raindrop size distribution (DSD) approach or the comparison of radar rainfall and rain gauge data. Typically, its functional form assumes a power law equation (e.g. Battan 1973), but it can also be provided as a look-up table (e.g. Rosenfeld *et al.* 1994) acquired by statistically matching rain gauge and radar reflectivity data.

Significant rainfall accumulation errors that arise from the temporal gaps of radar sampling can be corrected by accounting for the estimated storm movement (e.g. Fabry *et al.* 1994; Liu & Krajewski 1996). In Hydro-NEXRAD, Fabry *et al.*'s (1994) method is used. Reflectivity thresholds are used to distinguish rain from no-rain and to mitigate the effect of hail contamination on rainfall estimates.

Merging data from multiple radars

Certain limitations that might arise from using single radar data (i.e. beam blockage, limited coverage and vertical gaps between elevation angles) can be mitigated by combining (merging) data from two or more radars. One primary consideration in multiple radar data merging is whether to combine reflectivity or the converted rainfall maps to better represent rainfall over a specific area of interest. As WSR-88D radars are not synchronized, constructing reflectivity data mosaics requires temporal synchronization and spatial transformation techniques (e.g. Zhang *et al.* 2005; Lakshmanan *et al.* 2006; Langston *et al.* 2007). On the other

hand, rainfall data mosaics (e.g. Baldwin & Mitchell 1997; Fulton *et al.* 1998) have been obtained primarily by using hourly rainfall accumulations and the HRAP (Hydrologic Rainfall Analysis Project; see Reed & Maidment 1999) projection grid. However, radar data inconsistency due to calibration differences (e.g. Anagnostou *et al.* 2001; Gourley *et al.* 2003; Zhang *et al.* 2005) among WSR-88D radars pose the most significant challenge. Depending on the spatial interpolation scheme used in merging radar data, these differences can be clearly visible (for more detail, see Zhang *et al.* 2005). In Hydro-NEXRAD, we implemented both reflectivity and rainfall data merging options (called data- and product-based merging, respectively). The latter option accommodates a weighting function that describes the uncertainty of estimated rainfall amounts (see Ciach *et al.* 2007).

The next section delineates the overall modular architecture of the system. We first describe single radar data processing and rainfall estimation and distinguish data ingest and three major steps for modular components: reflectivity data processing, rainfall product generation and geo-referencing. Several modules are involved in these steps, and they may or may not be invoked. We discuss radar-rainfall estimation algorithms in the third section, using the operational NWS WSR-88D rainfall estimation algorithm called the Precipitation Processing System (PPS) (Fulton *et al.* 1998) as a springboard. Subsequently, the fourth section introduces two options for merging data from multiple radars. Finally, the last section summarizes and discusses the Hydro-NEXRAD system's advantages and potential benefits and delineates its limitations.

MODULAR ARCHITECTURE OF THE SYSTEM

Overview

The Hydro-NEXRAD system's functionality is achieved by processing data archived in the Hydro-NEXRAD databases. The main database tracks the data ingest and status. This database, populated while volume scan data are ingested, is complemented by the metadata information (see Kruger *et al.* 2011) stored in a different relational database. These procedures, illustrated in Figure 1, are defined as 'data ingest'. During the data ingest step, Hydro-NEXRAD automated utilities convert raw data files to an efficient data format –

an ASCII Run Length Encoding (RLE; see Kruger & Krajewski 1997) – after verifying readability, completeness and self-consistency of the files. Metadata are also computed at this stage (Kruger *et al.* 2011). Data ingest takes place prior to making data available to Hydro-NEXRAD users. The project's principal investigators decided which data to include in the Hydro-NEXRAD system (see e.g. Krajewski *et al.* 2011). While these decisions were largely arbitrary, they were responsive to community demands. Once populated with data, the Hydro-NEXRAD system becomes available to users, and the converted and database-indexed files become available for further processing in Hydro-NEXRAD. While users order the available data and derived products, the process of data ingest continues independently, thus increasing the size of the dataset that is available for future use. Data ingest in the Hydro-NEXRAD system was halted in 2008 (see Krajewski *et al.* 2011) when the federal agencies that operate the NEXRAD system switched data acquisition to the super-resolution mode (Istok *et al.* 2009).

Construction of the available products involves volume scan data processing to provide reflectivity and/or rainfall
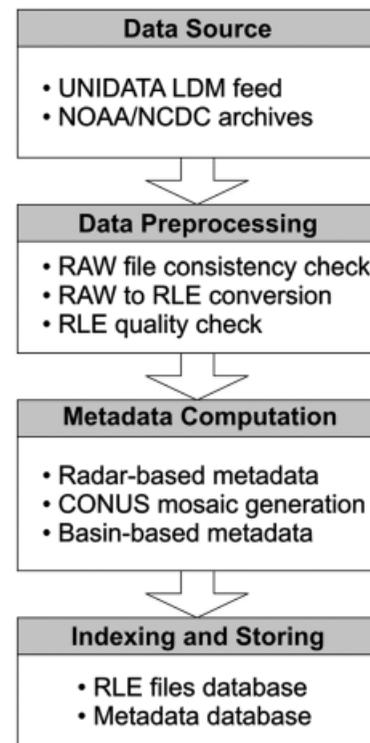

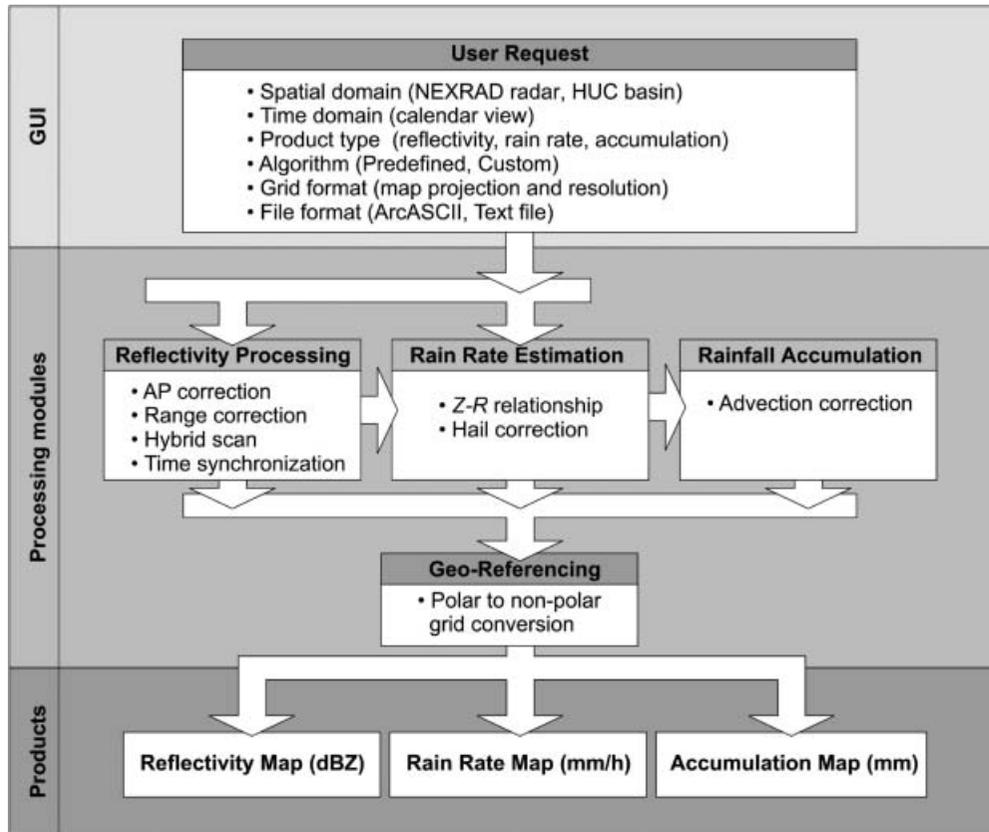**Figure 1** | Hydro-NEXRAD data ingest procedures.

Figure 2 | Modular architecture of the Hydro-NEXRAD system.

products, as shown in Figure 2. The optional modules for reflectivity data processing remove data contaminated by ground clutter and anomalous propagation of the radar beam. This is referred to as data quality control. Other modules correct for range-dependent biases using an azimuth-dependent vertical reflectivity profile. The available reflectivity maps are constructed using a hybrid scan or a scan of the elevation angle data. The hybrid scan module assigns reflectivity values for each azimuth and range bin from the several lowest elevation angles by a range-dependent weighting function (kernel).

The rainfall rate module converts the quality-controlled reflectivity (dBZ) to rainfall intensity (mm/h) using a power–law relationship (Z–R). If rainfall accumulation maps are selected as a final product, the next step is to accumulate consecutive rainfall rate maps over specific time duration, ranging from 15 min to daily. The accumulation module mimics real-time processing and optionally corrects radar accumulation errors that occur as a result of an intermittent

temporal sampling problem by applying an advection correction procedure (Fabry et al. 1994).

Finally, grid conversion (geo-referencing) and product packaging modules are used to increase the utility of the generated products for hydrologic research and applications. Below, we briefly describe the main aspects of each step involved in the preparation of rainfall products available via the Hydro-NEXRAD system.

Data ingest

The Hydro-NEXRAD system has acquired Level II reflectivity data from the NOAA National Climatic Data Center (NCDC) archive and/or the Unidata Local Data Manager (LDM) real-time feed. The process consists of quality control checks on raw data files, conversion of the file format, the indexing of both raw and converted reflectivity data, and the computation and storage of metadata. A small percentage of raw Level II data files is corrupted during data collection

and/or transmission (Kelleher *et al.* 2007), rendering them impossible to read and/or interpret correctly. In Hydro-NEXRAD, we have automated several consistency checks to ensure that all files available for product generation can be read and interpreted correctly. Their header information is consistent with the file content.

The process is fully automated and implemented through 'crawlers,' defined as programs that continuously check volume data intervals, control the data (verified as good and consistent), and perform metadata calculations (for more detail, see Kruger *et al.* 2011). Radar data and accompanying metadata stored in the Hydro-NEXRAD system databases create the basis for generating rainfall products that can be customized to user specification. The following describes the available data processing steps, which can be included during the product ordering process. Product ordering takes place via an internet browser based Graphical User Interface (GUI; see Krajewski *et al.* 2011). Selections made via the GUI constitute a set of job order commands and are interpreted by the Hydro-NEXRAD software into a sequential execution of a number of modular executables. Each unique organization of modules used represents a separate radar-rainfall estimation algorithm of the Hydro-NEXRAD system.

Reflectivity data processing

Anomalous Propagation (AP) identification

The approach proposed by Steiner & Smith (2002) is applied to classify the volume scan radar reflectivity data into precipitation and non-precipitation echoes. While the non-precipitation echo may include ground clutter as well as non-meteorological targets (e.g. airplanes, birds, etc.), the method searches for precipitation-like echo structures. The procedure constructs a 3D structure using reflectivity volume data and estimates 'the likelihood of atmospheric conditions' indicative of AP occurrence by evaluating such decision factors as 'the vertical extent of radar echoes,' 'their spatial variability,' and 'the vertical gradient of intensity.' The final classification map is obtained on a 2D polar grid. All pixels above a pixel classified as a non-precipitation echo at the lowest elevation angle are also classified as such. A 2D polar grid binary mask is constructed and used in subsequent modules.

Hybrid scan

Reflectivity products include the entire 3D volume scan or a 2D reflectivity map. To construct a reflectivity map, depending on a user's preference, the module can simply use one of the elevation angle (EA) data or produce an amalgam of several lowest elevation angle data, called a hybrid scan. Prior to applying the procedure, all volume scan reflectivity data are remapped onto a fixed polar grid with resolution of 1° by 1 km in radial azimuth and range, respectively. To construct a hybrid scan, a CAPPI (Constant Altitude Plan Position Indicator) option uses a Gaussian or a log-normal kernel to assign the weight contribution of measured reflectivity at each elevation angle. The weight values acquired from a kernel function for a given range are normalized to total 1. Both kernel functions defined by a CAPPI height parameter (corresponding to the mean and the mode for the Gaussian and the log-normal distribution, respectively) alleviate the reflectivity or rainfall map discontinuity problem that frequently occurs between transition zones of elevation angles.

Figure 3 illustrates radar beam altitudes of the lowest four elevations and compares weight contributions among elevation angles for both kernels. Since data from lower elevation angles can often be contaminated with ground clutter, different kernel weightings can lead to the suppression or enhancement of false echoes. Preliminary analysis revealed that the log-normal distribution performs better than the Gaussian by assigning lower weights to lower elevation angles; thus, it has been selected as the default option in the Hydro-NEXRAD system.

As an example case, Figure 4 shows that sharp boundaries can be observed in the PPS-produced reflectivity and rainfall maps (left) where elevation angles switch. In Hydro-NEXRAD, these sharp boundaries can be removed by using the CAPPI option that uses a smoothing kernel, as seen in Figure 4 (right). For completeness and comparison, we also include an option to use the hybrid scan defined in Fulton *et al.* (1998). This allowed the comparison of the discussed effects with respect to the NWS products.

Range effect correction

Range-dependent biases, radar sampling volume augmentation, and beam degradation with respect to the increase of distance from the radar usually yield a significant
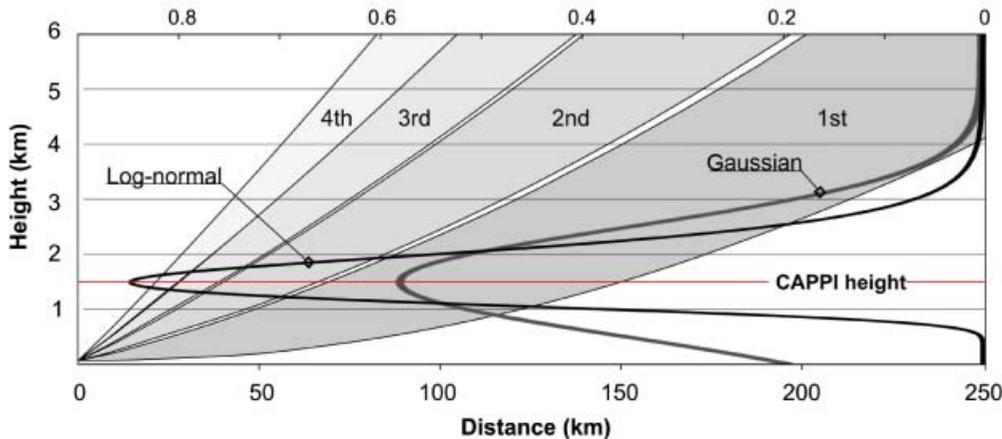
Figure 3 | Radar beam altitudes of the lowest four elevation angles and their contribution to the construction of a CAPPI by kernel weights. Two kernels (Gaussian and log-normal) are provided as an example for a 1.5 km CAPPI height above the radar altitude. The log-normal kernel decreases rapidly in the altitudes near the ground so that the weight contribution of the lowest radar elevation angle in log-normal kernel is relatively much smaller than in the Gaussian kernel.

underestimation in rainfall amounts. This effect can be mitigated by using a vertical profile of reflectivity (VPR, e.g. see Kitchen *et al.* 1994; Andrieu & Creutin 1995; Joss & Lee 1995; Vignal *et al.* 1999; Vignal & Krajewski 2001) obtained from a 3D reflectivity structure. In Hydro-NEXRAD, the modified VPR method of Vignal & Krajewski (2001) aggregates every volume of data within a 1 hour duration from the current time stamp to estimate hourly azimuth-dependent VPRs. The hourly VPRs are also updated every 5–10 min whenever a new volume of data is acquired. This hourly estimation of VPRs enables a real-time operational approach. As demonstrated in the literature, the VPR correction often effectively mitigates radar measurement errors caused by a bright band as well as by radar beam degradation due to cloud overshooting (e.g. Kitchen *et al.* 1994; Vignal *et al.* 1999; Zhang *et al.* 2008).

Rainfall products generation

Generation of rainfall products invokes several modules that include rainfall rate and rainfall accumulation calculation. In this section, we describe major modules of the single radar data processing. We will describe products merged from data from two or more radars in the next section.

Z–R relationship

Radar reflectivity, Z (mm^6/mm^3), is related to the power of electromagnetic waves backscattered from raindrops.

Rainfall intensity or rate, R (mm/h), from reflectivity measurements is determined by an empirical reflectivity-rainfall (Z–R) relationship, which one can model using a power law ($Z = aR^b$) relationship (Marshall & Palmer 1948; Krajewski & Smith 2002). In Hydro-NEXRAD, a user can not only select from three common Z–R relationships: 'NEXRAD' with $a = 300$ and $b = 1.4$ (Fulton *et al.* 1998), 'Tropical' with $a = 250$ and $b = 1.2$ (Rosenfeld *et al.* 1993), and 'Marshall–Palmer' with $a = 200$ and $b = 1.6$ (Marshall & Palmer 1948), but he or she can also specify custom values for the two variables (a and b) of the power relationship.

Hail correction

Occasionally, hail cores in thunderstorms may lead to unreasonable rainfall intensity after using the empirical Z–R power law conversion. The 'hail cap' threshold applied in the module defines the maximum instantaneous rainfall intensity. The typical threshold value for NEXRAD was defined as 104 mm/h corresponding to 53 dBZ (Fulton *et al.* 1998). This is a default value in Hydro-NEXRAD, but it is also an adaptable parameter that users can specify at different values.

Advection correction

The impact of rainfall accumulation errors caused by the temporal sampling span of rain fields might be even more significant than that of other error sources. The procedure
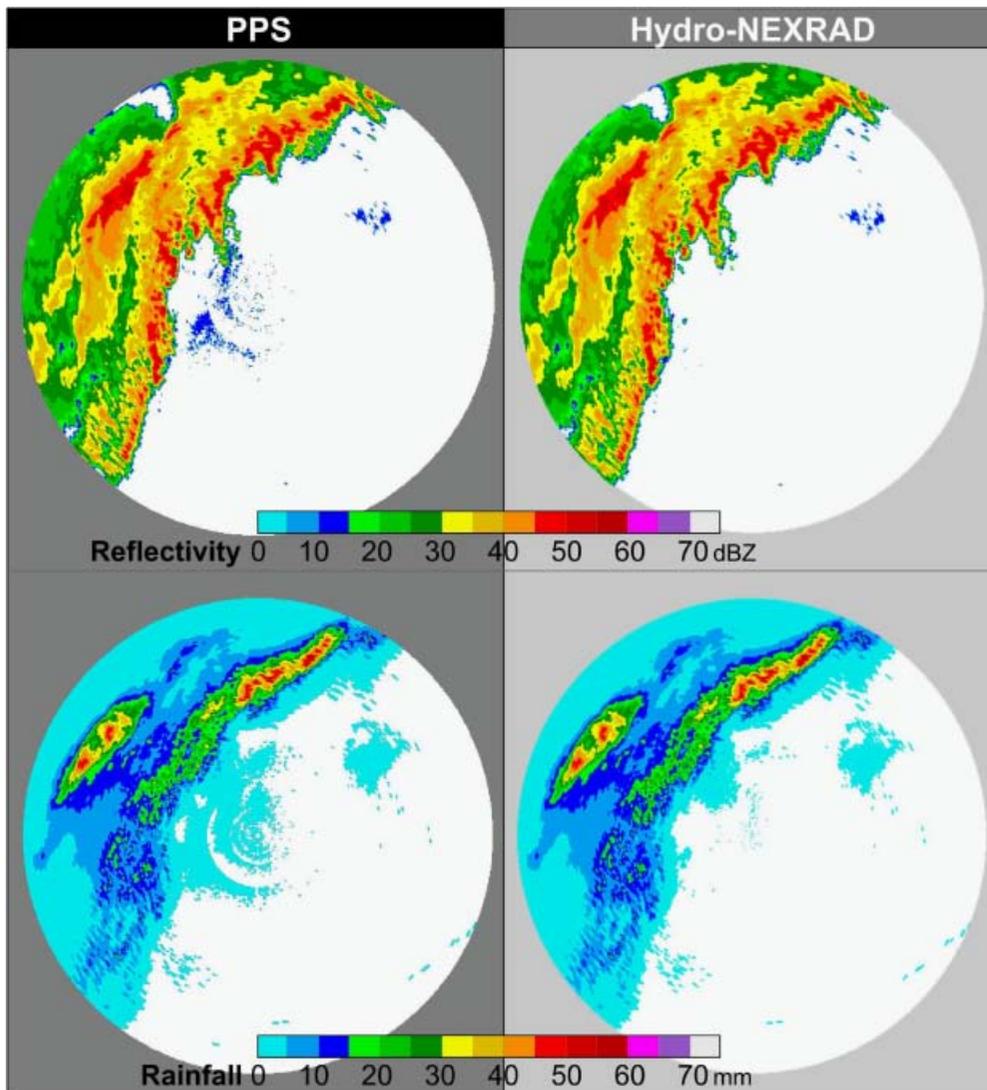
Figure 4 | Hybrid scan reflectivity maps (upper) at 0856 UTC 02 October 1998 and 1-hour rainfall maps (lower) ending at 0900 UTC 02 October 1998 from the Oklahoma City WSR-88D (KTLX), OH. The CAPPI hybrid scan (right) removes a discontinuity problem, while the hybrid scan in the PPS (left) shows several rings at transition zones of elevation angles.

applied in Hydro-NEXRAD is based on the approach proposed by Fabry *et al.* (1994). For every two consecutive reflectivity maps converted to the Cartesian domain, velocity vectors are computed using a cross-correlation method. Considering the short time interval (5–10 min) between the maps, the assumptions that the velocity of precipitation fields is constant and that the linear intensity changes are both reasonable. Once the conditions that describe the existence of precipitation fields and non-zero velocity vectors are detected, velocity vectors can be used to produce interpolated intermediate reflectivity maps. The default configuration

allows the generation of precipitation fields with one minute intervals. Such high temporal resolution can provide enhanced accuracy of rainfall estimation. Users can select whether or not advection correction should be applied, as it significantly increases the amount of time required for data processing and delivery.

Rainfall accumulation

The integration of successive rainfall rate maps over a specific time interval, such as 15 min or 1 hour, is applied to accu-

mulate rainfall amounts over a $1°$ by 1 km resolution, polar grid system. The module totals rainfall amounts of all periods (a period is defined as two successive rainfall rate maps over 5–10 minutes) within the accumulation interval requested by a user. If the proportion of a missing time period exceeds 10% of the user-requested accumulation interval, no accumulation product is produced. At the user's request, daily (or 24 hour) rainfall totals can be produced based on hourly accumulation maps. Daily accumulation starts at 1200 UTC (Coordinated Universal Time) as a default parameter.

Geo-referencing

User-defined rainfall products requested for a single radar are prepared using the fixed 2D polar grid centered on the radar. In the final step of the product generation, the radar-centered products are remapped to a projected grid for the subsequent hydrologic applications. When ordering data for the United States Geologic Survey (USGS) Hydrologic Unit (HU; see e.g. Seaber *et al.* 1987) selected by the user, the final product is provided for a Lat/Lon box that completely includes the unit when the unit is completely covered by a single radar umbrella. Units that are small compared to the entire radar umbrella (as is the case for most eight digit HU Codes), require processing of the volume scan data for a limited sector only, thereby significantly reducing the processing time.

Since different hydrologic applications require various resolution precipitation data, Hydro-NEXRAD provides several options for a final product grid selection. A short description of available grid formats follows. The NWS developed a polar stereographic projection called HRAP (Hydrologic Rainfall Analysis Project) for their official radar-rainfall products (see e.g. Fulton *et al.* 1998). HRAP is a quasi-rectangular grid that has a nominal grid spacing of 4×4 km^2. Based on the HRAP projection (Reed & Maidment 1999), we have developed the S-HRAP (for Super HRAP) as a finer HRAP grid with a nominal resolution of 1×1 km^2. It uses the same projection as HRAP but with 4×4 times higher resolution. Hydro-NEXRAD also provides products at the Land Data Assimilation System (LDAS) grid (Mitchell *et al.* 1999), that is, a 1/8 degree of latitude and longitude grid, commonly used by the satellite remote sensing community. In addition, a Lat/Lon geographic grid with approximately 2 km $\times$ 2 km

$(1' \times 1')$ resolution is offered to avoid distortion caused by map projections. When multiple radar products are desired, the 2 km $\times$ 2 km $(1' \times 1')$ grid is used for merging radar reflectivity or rainfall onto a common grid.

RAINFALL PROCESSING ALGORITHMS

Hydro-NEXRAD uses the aforementioned modules to produce rainfall products according to user-specified algorithms. Hydro-NEXRAD has one customizable and three predefined (Quick Look, Hi-Fi, and Pseudo NWS PPS; Fulton *et al.* 1998) algorithms, as presented in Figure 5. The Quick Look is the fastest algorithm, implying that no AP, range or advection correction for reflectivity processing is applied. Conversely, all corrections are performed in the Hi-Fi algorithm to mitigate the negative effects of corresponding error sources as a consequence, significantly more processing time is needed.

The pseudo NWS PPS algorithm is the Hydro-NEXRAD implementation of the NWS PPS algorithm (Fulton *et al.* 1998). We refer to it as 'pseudo' because it does not reproduce exactly the same official NWS products. It uses the hybrid scan constructed by the nearest angle data to 1 km above the radar altitude. The differences between the 'official' PPS and the Hydro-NEXRAD pseudo PPS stem from the lack of the stand alone source code available outside of the NEXRAD agencies. The known differences include terrain maps used on radar beam blockage map construction and the AP detection procedure. The PPS AP procedure uses Doppler information not included in the Hydro-NEXRAD database.

The customizable algorithm enables expert users to select options that they consider the best for their specific application. These include reflectivity versus rainfall rate relationship, hybrid scan height, and mix-and-match choice of corrective algorithms for AP detection, advection, and range effect.

MULTIPLE RADAR MERGING OPTIONS

When a user selects a basin that is covered by more than one radar, merging of data from multiple radar may be invoked. Multiple radar data merging in Hydro-NEXRAD involves

		Custom	Quick Look	Hi-Fi	Pseudo NWS PPS
Quality Control	AP Correction	Yes/No	No	Yes	No
	Range Correction	Yes/No	No	Yes	No
	Hybrid Scan	CAPPI, PPS, EA	CAPPI	CAPPI	PPS
Rain Rate Conversion	Power Law Z–R	ND, MP, TL, CM	ND	ND	ND
Rainfall Accumulation	Advection Correction	Yes/No	No	Yes	No

Figure 5 │ Hydro-NEXRAD radar-rainfall algorithm combinations: Custom, Quick Look, Hi-Fi, and pseudo NWS PPS. For power–law Z–R, 'ND,' 'MP,' 'TL,' and 'CM' represent 'NEXRAD,' 'Marshall–Palmer,' 'Tropical,' and 'Custom', respectively.

two options: (1) data-based merging, and (2) product-based merging. The merging procedures related to module sequence and data feed at each step are illustrated in Figure 6. We provide both of these options as it is difficult to say *a priori* which approach leads to better final results. Following the principle of correct averaging order for non-linear operations (such as radar-rainfall estimation), option (2) should be better. However, some studies (e.g. Ciach *et al.* 1997) indicate that the difference is negligible. Also, for optimal estimation of the final product, proper averaging would require knowledge of the range dependent structure of uncertainties of the averaged quantities. Such knowledge is generally unavailable.

Data-based merging

As mentioned in the previous section, the merging procedure based on radar volume data performs reflectivity data processing according to a user-requested algorithm for all radars involved in a user-specified hydrologic unit, produces data every 5 min to synchronize the temporal scale between individual radar data to be merged, and finally combines data onto a common grid, as shown in Figure 6. Reflectivity

values for a given location are assigned by a weighting function that describes their contributions with respect to the distance from available radars. This single reflectivity field is then converted to rainfall amounts according to the user-requested algorithm.

Common grid

The WSR-88D radars collect their raw observations based on a spherical coordinate system represented by the range, azimuth, and elevation angle plane. Since single radar data cannot be combined using this local spherical coordinate, a common framework is needed to merge the individual data-sets. Earlier studies (e.g. Zhang *et al.* 2005; Lakshmanan *et al.* 2006; Langston *et al.* 2007) used a polar-to-Cartesian coordinate translation to merge multi-radar data. In Hydro-NEXRAD, we define $2 \text{ km} \times 2 \text{ km}$ ($1' \times 1'$) geographic coordinates as a reference common grid to avoid distortions related to Cartesian grids, especially at large-scale domains. The advantage of using geographic coordinates is that product maps can be easily transformed into other grid formats such as LDAS, HRAP, and S-HRAP that are provided in the Hydro-NEXRAD system.
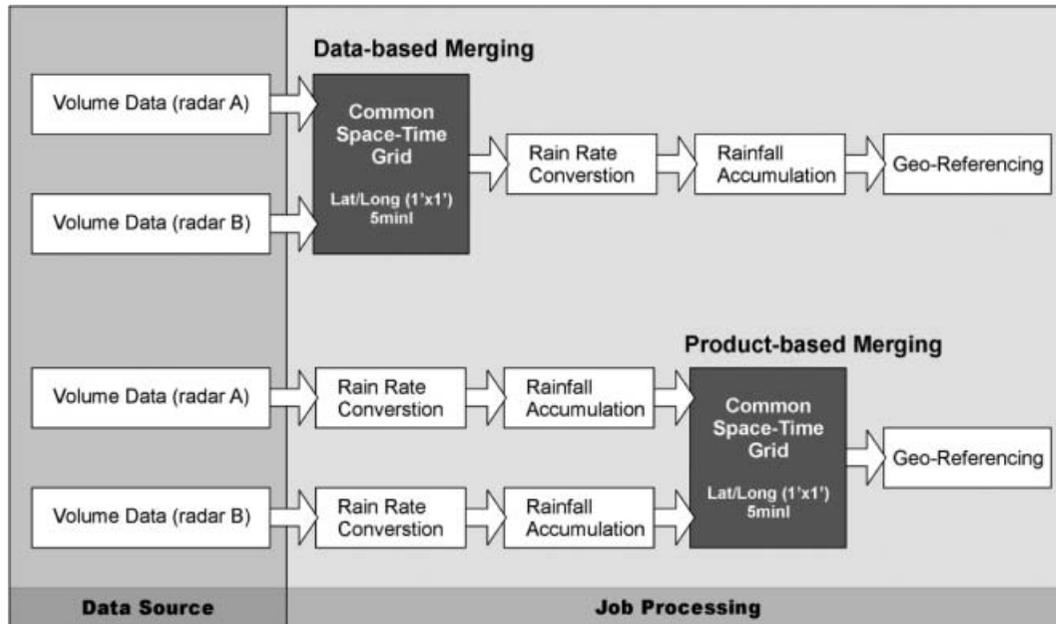
Figure 6 | Processing procedures of multiple radar merging options in Hydro-NEXRAD: data- and product-based merging.

Temporal synchronization

As WSR-88D radars are not operationally synchronized, reflectivity data from multiple radars require temporal synchronization, as shown in Figure 7 (top), before they can be combined. An exponentially decaying weighting function (Langston et al. 2007) is used to consider temporal variations of multiple radar data. The time interval of consecutive volume scans is dependent on the Volume Coverage Pattern (VCP) and ranges from 4 to 10 min. Therefore, one should consider a proper parameter value for longer scan strategies because temporal weight may go to zero for some parameter values when the time interval is close to 10 min. We use 5 min as the time scale parameter value to temporally synchronize multiple radar volume data acquired at different times. The weight values obtained from the double exponential function are normalized to total 1.

Spatial merging

Due to radar beam spreading and differences in reflectivity from multiple radar data, it is reasonable to allow values from closer ranges to have more weight than those from farther ranges in order to reduce radar beam overshooting problems,

as shown in Figure 7 (bottom). Although using a weighting function is not an optimal solution when dealing with calibration differences among radars, it can lessen the effect of the differences and serves as an alternative to the nearest neighborhood method (Zhang et al. 2005). A 'steep weighting function (rapidly decreasing weight)' with respect to distance is necessary since increasing the sampling volume at far ranges might smooth the structure of severe storms (Zhang et al. 2005). We also use the double exponentially decaying weighting function (Langston et al. 2007) to spatially combine multiple radar data. We use 25 km as the length scale parameter value.

Figure 8 shows an example case of individual radar (top and middle) and merged (bottom) reflectivity maps for Middle and Lower Iowa River watersheds monitored by Des Moines and Davenport WSR-88D radars (KDMX and KDVN, respectively). Since the distance from radars plays a significant role when combining reflectivity values from individual radars, distance ranges (each circle represents a 50 km range) from both radars are illustrated in Figure 8. The merged reflectivity structure demonstrates that reflectivity values in the merged plane are more affected by closer radar because of the use of the steep weighting function.
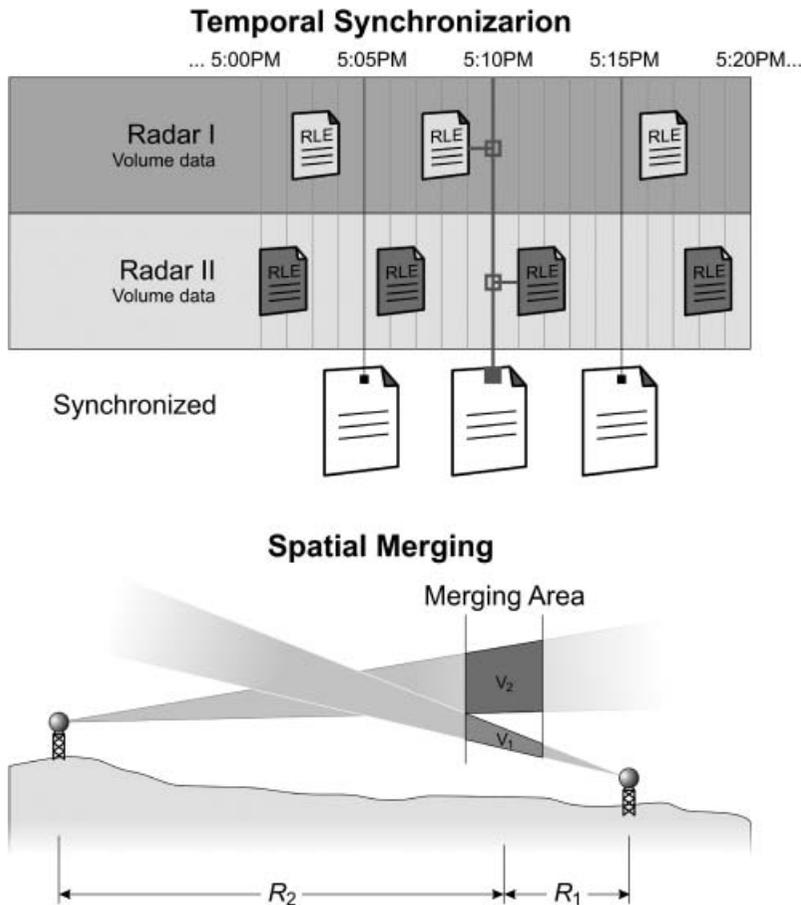
Figure 7 │ A schematic showing temporal synchronization and spatial merging of multiple radar data merging.

Product-based merging

Most of the current multi-sensor approaches (e.g. Seo *et al.* 2005; Zhang *et al.* 2005; Lakshmanan *et al.* 2006; Langston *et al.* 2007) produce only deterministic precipitation fields. It is indisputable that rainfall estimates from remote sensors are highly variable due to the lack of understanding of the relevant physical processes in a specific domain of time and space and the observation system itself. However, those multi-sensed products do not provide any quantitative information about the uncertainty of rainfall products.

When product-based merging is implemented in Hydro-NEXRAD, reflectivity data from multiple radars are all converted to rainfall accumulations using a user-specified algorithm, as described in the previous section. A user-specified algorithm is connected with proper components (modules) of the system, which are radar reflectivity

quality control and processing, rainfall rate conversion, and rainfall accumulation, as shown in Figure 6. This is repeated for all radars involved. These products are then converted onto a common Lat/Lon grid and combined into the final product using a weighting function that describes the uncertainty of estimated rainfall amounts (Ciach *et al.* 2007). Finally, the merged product given on the common Lat/Lon grid can be converted to other grid formats (i.e. LDAS, HRAP, and S-HRAP) for subsequent hydrologic research and applications.

Individual (upper) and two merged (lower) rainfall maps for the same event as shown in Figure 8 are presented in Figure 9. The map from the product-based merging indicates that rainfall strength tends to be lower than in individual maps because the overall bias factor (less than 1.0 for the hot season) is eliminated before combining individual maps using the uncertainty component defined by the distance zones (for
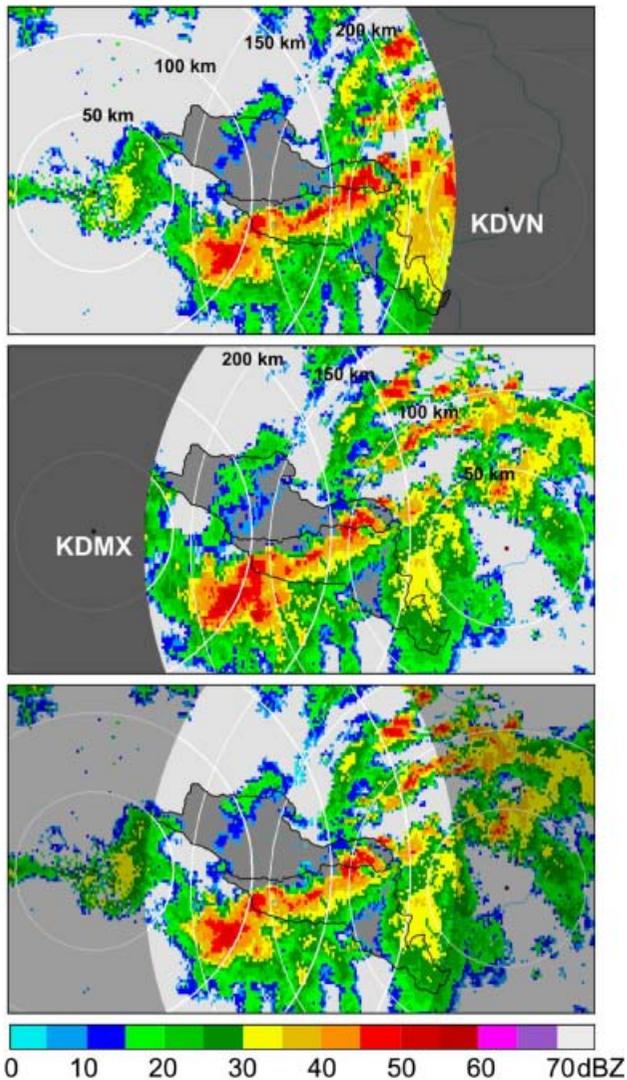
NEXRAD system given in Krajewski *et al.* (2011) and the description of the metadata that allows users of the system to select hydrologically relevant cases (Kruger *et al.* 2011). The novelty of the Hydro-NEXRAD system is not in the algorithms used but in the overall structure and organization of the service it provides to the hydrologic research community.

The Hydro-NEXRAD system allows users to focus on specification of rainfall product requirements, without being burdened by radar-specific, technical issues. Proper assessment of many of these issues requires considerable expertise and experience in the physics of radar observational process, radar hardware issues, radar data processing, and estimation (i.e., uncertainty) issues. Since expecting all users to have such expertise is unreasonable, Hydro-NEXRAD shields users whose focus is on hydrologic processes from the details of radar-rainfall estimation. At the same time, expert users may specify many of the parameters according to their own knowledge, experiences, and expectations. Still, there are many choices and decisions that we have made in the implementation of the algorithms described herein that, while not fundamental, might affect the final products.

Based on the preliminary comparisons we have performed (e.g. Seo & Krajewski 2010), as well as the feedback we have received from the system users (e.g. Villarini & Krajewski 2010), the products generated by the system are similar in accuracy and precision to other products (e.g. Fulton *et al.* 1998) available for the same (or similar) space and time resolution. While we cannot say the same for products at other resolutions (since they are not generally available from the NEXRAD agencies or other sources), the fact that we use a consistent set of algorithms to produce them makes us believe that these high-resolution products are as adequate. A comprehensive performance analysis of the Hydro-NEXRAD product is outside of the scope of this communication. We are conducting such comprehensive analysis and will report its results soon.

There are many advantages of the Hydro-NEXRAD modular structure. Users representing different research and engineering communities can custom specify rainfall products that satisfy their specific purposes. We also hope that experts will contribute their algorithms to be included with the original ones we selected.
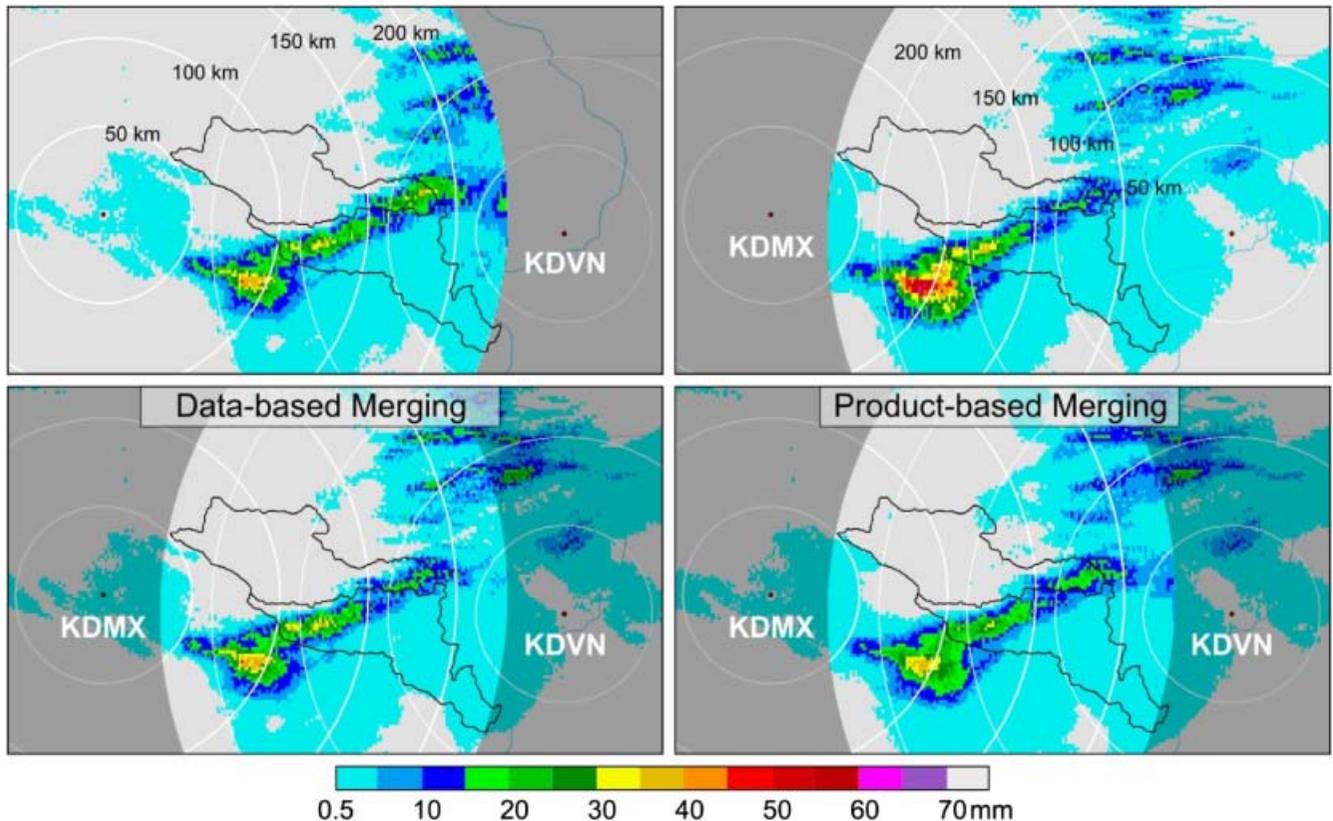

Figure 8 | Individual (top and middle) and merged (bottom) reflectivity maps at 0130 UTC 26 July 2006 from the KDMX and the KDVN. Each circle represents a 50 km range from the radars.

more detail, see Ciach *et al.* 2007). In addition, the rainfall map of data-based merging produced from merged reflectivity maps shows little difference from that of the product-based merging.

SUMMARY AND DISCUSSION

In this paper, we presented modules and algorithms used for Level II NEXRAD data processing for rainfall estimation. This paper complements the overview of the Hydro-

Figure 9 │ Individual (upper) and merged (lower) 1 hour rainfall maps at 0200 UTC 26 July 2006 from the KDMX and the KDVN.

One of the most important advantages of the Hydro-NEXRAD system is the repeatability of results. Two users who specify the same algorithms in Hydro-NEXRAD will obtain exactly the same results. This is in contrast to the current practice where it is difficult to reproduce exactly the results published by others (e.g. Fulton *et al.* 1998). The Hydro-NEXRAD system has a modular design, and it is relatively easy to add more options as modules to the system. For example, one could add different AP detection, range correction, or advection correction algorithms. Therefore, Hydro-NEXRAD has the potential to serve as a community resource for the future development of radar-based rainfall estimation.

Perhaps the most significant practical challenge for the multiple radar data merging is the fact that the WSR-88D radars are not cross calibrated, and there is lack of information on the absolute calibration procedures and schedule. We hope that joint community efforts, such as that described by Vasiloff *et al.* (2007), will help to overcome this limitation.

At this point, all Hydro-NEXRAD products are radar-based only. Merging of Hydro-NEXRAD products with rainfall data from other sources (e.g. rain gauges and satellites) has not been in the scope of the presented effort. While there are many methods documented in the literature for merging radar and rain gauge data (e.g. Krajewski 1987; Creutin *et al.* 1988; Seo 1998; Todini 2001; Velasco-Forero *et al.* 2009), the main obstacle in their implementation is the generally poor quality of the rain gauge data. Also, the abundance of the networks operated by many different organizations poses a challenge to the uniformity of the data quality.

and Radoslaw Goska who coded the scripts that connect the Graphical User Interface and the algorithmic modules.

REFERENCES

Anagnostou, E. N., Morales, C. A. & Dinku, T. 2001 The use of TRMM precipitation radar observations in determining ground radar calibration biases. *J. Atmos. Oceanic Technol.* **18**(4), 616–628.

Andrieu, H. & Creutin, J. D. 1995 Identification of vertical profiles of radar reflectivity for hydrological applications using an inverse method. Part I: Formulation. *J. Appl. Meteor.* **34**(1), 225–239.

Austin, P. M. 1987 Relation between measured radar reflectivity and surface rainfall. *Mon. Wea. Rev.* **115**(5), 1053–1070.

Austin, P. M. & Bemis, A. C. 1950 A quantitative study of the bright band in radar precipitation echoes. *J. Meteor.* **7**(2), 145–151.

Baldwin, M. & Mitchell, K. 1997 The NCEP hourly multi-sensor U.S. precipitation analysis for operations and GCIP research. *Preprint, 13th conf. on Hydrology*, Long Beach, CA, Amer. Meteor. Soc., 54–55.

Battan, L. J. 1973 *Radar Observation of the Atmosphere.* The University of Chicago Press, Chicago, IL.

Berenguer, M., Sempere-Torres, D., Corral, C. & Sánchez-Diezma, R. 2006 A fuzzy logic technique for identifying nonprecipitating echoes in radar scans. *J. Atmos. Oceanic Technol.* **23**(9), 1157–1180.

Cho, Y.-H., Lee, G. W., Kim, K.-E. & Zawadzki, I. 2006 Identification and removal of ground echoes and anomalous propagation using the characteristics of radar echoes. *J. Atmos. Oceanic Technol.* **23**(9), 1206–1222.

Chumchean, S., Seed, A. & Sharma, A. 2004 Application of scaling in radar reflectivity for correcting range-dependent bias in climatological radar rainfall estimates. *J. Atmos. Oceanic Technol.* **21**(10), 1545–1556.

Ciach, G. J., Krajewski, W. F., Anagnostou, E. N., Baeck, M. L., Smith, J. A., McCollum, J. R. & Kruger, A. 1997 Radar rainfall estimation for ground validation studies of the Tropical Rainfall Measuring Mission. *J. Appl. Meteor.* **36**(6), 735–747.

Ciach, G. J., Krajewski, W. F. & Villarini, G. 2007 Product-error-driven uncertainty model for probabilistic quantitative precipitation estimation with NEXRAD data. *J. Hydrometeor.* **8**(6), 1325–1347.

Creutin, J. D., Delrieu, G. & Lebel, T. 1988 Rain measurement by raingage-radar combination: A geostatistical approach. *J. Atmos. Oceanic Technol.* **5**(1), 102–115.

Doviak, R. J. & Zrnic, D. S. 1993 *Doppler Radar and Weather Observations.* Academic Press, (Second Edition), San Diego, CA.

Ellis, S., Kessinger, C., O'Bannon, T. D. & VanAndel, J. 2003 Mitigating ground clutter contamination in the WSR-88D. *19th International Conference on Interactive Information and Processing Systems (IIPS) for Meteorology, Oceanography, and Hydrology*, Long Beach, California, 9–13 February 2003.

Fabry, F., Bellon, A., Duncan, M. R. & Austin, G. L. 1994 High resolution rainfall measurements by radar for very small basins: the sampling problem re-examined. *J. Hydrol.* **161**(1–4), 415–428.

Fabry, F. & Zawadzki, I. 1995 Long-term radar observations of the melting layer of precipitation and their interpretation. *J. Atmos. Sci.* **52**(7), 838–851.

Fulton, R. A., Breidenbach, J. P., Seo, D.-J., Miller, D. A. & O'Bannon, T. 1998 The WSR-88D rainfall algorithm. *Wea. Forecasting* **13**(2), 377–395.

Gourley, J. J. & Calvert, C. M. 2003 Automated detection of the bright band using WSR-88D radar data. *Wea. Forecasting* **18**(4), 585–599.

Gourley, J. J., Kaney, B. & Maddox, R. A. 2003 Evaluating the calibrations of radars: A software approach. *Preprints, 31st International Conference on Radar Meteorology*, Seattle, Washington, 6–12 August 2003.

Grecu, M. & Krajewski, W. F. 2000 An efficient methodology for detection of anomalous propagation echoes in radar reflectivity data using neural networks. *J. Atmos. Oceanic Technol.* **17**(2), 121–129.

Istok, M., Fresch , M. A., Smith, S. D., Jing, Z., Murnan, R., Ryzhkov, A. V., Krause, J., Jain, M. H., Ferree, J. T., Schlatter, P. T., Klein, B., Stein, D. J., Cate, G. S. & Saffle, R. E. 2009 WSR-88D Dual polarization initial operational capabilities. Preprints, 25th Conf. on International Interactive Information and Processing Systems (IIPS) for Meteorology, Oceanography, and Hydrology, Phoenix, Amer. Meteor. Soc., Paper 15.5. http://ams.confex.com/ams/pdfpapers/148927.pdf.

Joss, J. & Lee, R. 1995 The application of radar-gauge comparisons to operational precipitation profile corrections. *J. Appl. Meteor.* **34**(12), 2612–2630.

Kelleher, K. E., Droegemeier, K. K., Levit, J. J., Sinclair, C., Jahn, D. E., Hill, S. D., Mueller, L., Qualley, G., Crum, T. D., Smith, S. D., Del Greco, S. A., Lakshmivarahan, S., Miller, L., Ramamurthy, M., Domenic, B., & Fulker, D. W. 2007 A real-time delivery system for NEXRAD Level II data via the internet. *Bull. Amer. Meteor. Soc.* **88**(7), 1045–1057.

Kessinger, C., Ellis, S. & VanAndel, J. 2003 The radar echo classifier: A fuzzy logic algorithm for the WSR-88D. *Preprints-CD, 3rd Conference on Artificial Intelligence Applications to the Environmental Sciences*, Long Beach, California, 9–13 February 2003.

Kitchen, M., Brown, R. & Davies, A. G. 1994 Real-time correction of weather radar data for the effects of bright band, range and orographic growth in widespread precipitation. *Quart. J. Roy. Meteor. Soc.* **120**(519), 1231–1254.

Krajewski, W. F. 1987 Co-kriging radar-rainfall and rain gage data, *J. Geophys. Res.* **92**(D8), 9571–9580.

Krajewski, W. F., Kruger, A., Smith, J. A., Lawrence, R., Gunyon, C., Goska, R., Seo, B.-C., Domaszczynski, P., Baeck, M. L., Ramamurthy, M. K., Weber, J., Bradley, A. A., DelGreco, S. A. & Steiner, M. 2011 Towards better utilization of NEXRAD data in hydrology: An overview of Hydro-NEXRAD. *J. Hydroinformatics* **13**(2), 256–267.

Krajewski, W. F. & Smith, J. A. 2002 Radar hydrology: rainfall estimation. *Adv. Water Resour.* **25**(8–12), 1387–1394.

Kruger, A. & Krajewski, W. F. 1997 Efficient storage of weather radar data, *Software Practice and Experience* **27**(6), 623–635.

Kruger, A., Krajewski, W. F., Domaszczynski, P. & Smith, J. A. 2011 Hydro-NEXRAD: Metadata computation and use. *J. Hydroinformatics* **13**(2), 268–277.

Lakshmanan, V., Fritz A., Smith T., Hondl, K. & Stumpf G. 2007 An automated technique to quality control radar reflectivity data. *J. Appl. Meteorol. Climatol.* **46**(3), 288–305.

Lakshmanan, V., Smith, T., Hondl, K., Stumpf, G. J. & Witt, A. 2006 A real-time, three-dimensional, rapidly updating, heterogeneous radar merger technique for reflectivity, velocity, and derived products. *Wea. Forecasting* **21**(5), 802–823.

Langston, C., Zhang, J. & Howard, K. 2007 Four-dimensional dynamic radar mosaic. *J. Atmos. Oceanic Technol.* **24**(5), 776–790.

Liu, C. & Krajewski, W. F. 1996 A comparison of methods for calculation of radar-rainfall hourly accumulations, *Water Resour. Bull.* **32**(2), 305–315.

Marshall, J. S. & Palmer, W. McK. 1948 The distribution of raindrops with size. *J. Atmos. Sci.* **5**(4), 165–166.

Mitchell, K., Houser, P., Wood, E., Schaake, J., Tarpley, D., Lettenmaier, D., Higgins, W., Marshall, C., Lohmann, D., Ek, M., Cosgrove, B., Entin, J., Duan, Q., Pinker, R., Robock, A., Habets, F. & Vinnikov, K. 1999 GCIP Land Data Assimilation System (LDAS) project now underway. *Gewex News* **9**(4), 3–6.

Moszkowicz, S., Ciach, G. J. & Krajewski, W. F. 1994 Statistical detection of anomalous propagation in radar reflectivity patterns. *J. Atmos. Oceanic Technol.* **11**(4), 1026–1034.

Reed, S. M. & Maidment, D. R. 1999 Coordinate transformations for using NEXRAD data in GIS-based hydrologic modeling. *J. Hydrol. Eng.* **4**(2), 174–182.

Rosenfeld, D., Wolff, D. B. & Amitai, E. 1994 The window probability matching method for rainfall measurement with radar. *J. Appl. Meteor.* **33**(6), 682–693.

Rosenfeld, D., Wolff, D. B. & Atlas, D. 1993 General probability-matched relations between radar reflectivity and rain rate. *J. Appl. Meteor.* **32**(1), 50–72.

Seaber, P. R., Kapinos, F. P. & Knapp, G. L. 1987 Hydrologic Unit Maps: U.S. Geological Survey Water Supply Paper 2294.

Seo, B.-C. & Krajewski, W. F. 2010 Scale dependence of radar-rainfall uncertainty: Initial evaluation of NEXRAD's new super-resolution data, *J. Hydrometeor.* **11**(5), 1191–1198.

Seo, D.-J. 1998 Real-time estimation of rainfall fields using radar rainfall and rain gage data. *J. Hydrol.* **208**(1–2), 37–52.

Seo, D.-J., Breidenbach, J., Fulton, R., Miller, D. & O'Bannon, T. 2000 Real-time adjustment of range-dependent biases in WSR-88D rainfall estimates due to nonuniform vertical profile of reflectivity. *J. Hydrometeor.* **1**(3), 222–240.

Seo, D.-J., Kondragunta, C. R., Kitzmiller, D., Howard, K., Zhang, J. & Vasiloff, S. V. 2005 The national mosaic and multisensory QPE (NMQ) project-status and plans for a community testbed for high-resolution multisensory quantitative precipitation estimation (QPE) over the United States. *The 85th AMS Annual Meeting*, San Diego, California, 8–14 January 2005.

Smith, J. A., Seo, D.-J., Baeck, M. L. & Hudlow, M. D. 1996 An intercomparison study of NEXRAD precipitation estimates. *Water Resour. Res.* **32**(7), 2035–2045.

Steiner, M. & Smith, J. A. 2002 Use of three-dimensional reflectivity structure for automated detection and removal of non-precipitating echoes in radar data. *J. Atmos. Oceanic Technol.* **19**(5), 673–686.

Todini, E. 2001 A Bayesian technique for conditioning radar precipitation estimates to rain-gauge measurements. *Hydrol. Earth System Sci.* **5**(2), 187–199.

Vasiloff, S. V., Seo, D.-J., Howard, K. W., Zhang, J., Kitzmiller, D. H., Mullusky, M. G., Krajewski, W. F., Brandes, E. A., Rabin, R. M., Berkowitz, D. S., Brooks, H. E., Mcginley, J. A., Kuligowski, R. J. & Brown, B. G. 2007 Improving QPE and very short-term QPF: An initiative for a community-wide integrated approach. *Bull. Amer. Meteor. Soc.* **88**(12), 1899–1911.

Velasco-Forero, C. A., Sempere-Torres, D. Cassiraga, E. F. & Gómez-Hernández, J. J. 2009 A non-parametric automatic blending methodology to estimate rainfall fields from rain gauge and radar data. *Adv. Water Resour.* **32**(7), 986–1002.

Vignal, B., Andrieu, H. & Creutin, J. D. 1999 Identification of vertical profiles of reflectivity from volume scan radar data. *J. Appl. Meteor.* **38**(8), 1214–1228.

Vignal, B. & Krajewski, W. F. 2001 Large-sample evaluation of two methods to correct range-dependent error for WSR-88D rainfall estimates. *J. Hydrometeor.* **2**(5), 490–504.

Villarini, G. & Krajewski, W. F. 2010 Sensitivity studies of the models of radar-rainfall uncertainties. *J Appl. Meteorol. Climatol.*, **49**(2), 288–309.

Zawadzki, I. 1982 The quantitative interpretation of weather radar measurements. *Atmos.–Ocean* **20**(2), 158–180.

Zhang, J., Howard, K. & Gourley, J. J. 2005 Constructing three-dimensional multiple-radar reflectivity mosaics: Examples of convective storms and stratiform rain echoes. *J. Atmos. Oceanic Technol.* **22**(1), 30–42.

Zhang, J., Langston, C. & Howard, K. 2008 Brightband identification based on vertical profiles of reflectivity from the WSR-88D. *J. Atmos. Oceanic Technol.* **25**(10), 1859–1872.